Piezoreflectance study of Nb-doped MoS_2 single crystals

Kerista Sebayang[1] and MulaSigiro[2,*]
[1]Department of Physics, Faculty of Mathematics and Natural Sciences, University of Sumatera Utara, Medan 20155, Indonesia.
[2]Department of Physics Education, Faculty of Teacher Training and Education, Universitas HKBP Nommensen, Medan 20234, Indonesia.

* mulasigiro@gmail.com

Abstract. We have measured the temperature dependence of the spectral features in the vicinity of direct band-edge excitonic transition of the Nb-doped MoS_2 single crystals from 25 to 300 K using piezoreflectance (PzR). The energies and broadening parameters of the A and B excitons of the Nb-doped MoS_2 samples have been determined accurately via a detailed line shape fit of the PzR spectra. we can infer that the Nb ions are most likely intercalated between the van der Waals gap and stabilize the rhombohedral 3R phase of the MoS_2 crystal.

1. Introduction

Molybdenum disulphide MoS_2 belongs to the group IVA layer type transition metal dichalcogenides having C_7 type crystal structure which is formed of unit layers consisting of transition metal (Mo) atoms sandwiched by chalcogen (S) atoms [1]. The MoS_2 compound has been extensively investigated because of the possible practical application as a solid state lubricant and a catalyst for hydrodesulfurization (HDS) and hydrogen evolution reaction (HER) [2-4], photoelectrochemical solar cells [5-6] , and can also be synthesized in large scale by chemical vapor deposition [7-11]. The monolayer MoS_2 single crystal exhibits high luminous energy photoconversion efficiencies [12-13], excellent electrical [14-16] and optical performance [17, 18] compared to its bulky counterpart. The successful application of this semiconductor compound originates largely from the sandwich interlayer structure, loosely bound by the weak van der Waals forces, as evidenced by easy cleavage in the c-direction along which the S-Mo-S layers are stacked to form the crystal [1, 19]. There are two known polytypes of MoS_2 [1, 19]; two-layer hexagonal and three-layer rhombohedral termed 2H and 3R, respectively. Both have regular layered structures with six-fold trigonal prismatic coordination of the Mo atoms by the sulfur atoms within the layers; 2H-MoS_2 has two layers per unit cell stacked in the hexagonal symmetry and belongs to the space group D_6^4 while 3R-MoS_2 has three layers in the c-direction but has rhombohedral symmetry and belongs to the space group C_3^5 . Naturally occurring 3R-MoS_2 has been found to be consistently rich in certain minor elements such as Re, Nb etc [20]. The incorporation of the impurity will essentially influence the structure symmetry of MoS_2, this is the adoption of the polytype 3R-MoS_2. For Nb-doped MoS_2, the niobium substitutions improve the photocurrent gain much more slowly than in the case of rhenium [21]. Niobium dopants seems to serve more than just as an impurity donor, it is most likely that niobium transition ions can either substitute for the Mo metal ions interstitially or intercalate between the Vander Waals gap resulting in a distortion of crystal structure [20, 21]. The sandwich Nb ions create stronger bonds than the original van der Waals forces and transform the two-layer hexagonal MoS_2 (2H-MoS_2) into three-layer rhombohedral MoS_2 (3R-MoS_2). The transformation of 2H-MoS_2 into 3R-MoS_2 by doping with niobium is perhaps not too surprising as it has been found that naturally

occurring 3R-MoS_2 is consistently rich in certain minor elements such as Nb, Re etc [21]. Despite the potentially attractive fundamental research offered by Nb-doped MoS_2, very few studies concerning the influence of niobium dopant on the electrical and optical properties of the material have been reported.

In this study, we present piezoreflectance (PzR) measurements which has been proven to be useful in the characterization of semiconductors [22, 23] of Nb-doped MoS_2 which grown by chemical vapor transport method with I_2 as transport agent. An elaborate temperature dependence of the spectral features near the direct band-edge excitonic transitions of the Nb-doped MoS_2 in the range 25 to 300 K has been obtained. The derivative nature of modulation spectra suppresses uninteresting background effects and greatly enhances the precision in the determination of inter band excitonic transition energies. The sharper line shape as compared to the conventional optical techniques has enabled us to achieve a greater resolution and hence to detect weaker features. The PzR spectra are fitted with a form of the Aspnes equation of the fist derivative Lorenzian lineshape [23, 24]. From a detailed lineshape fit we are able to determine accurately the energies and broadening parameters of the excitonic transitions. The parameters which describe the temperature behaviour of excitonic transitions indicate that A-B, caused by interlayer interaction and spin-orbit splitting, correspond to excitonic transitions with different origin. The origin of A, B excitons and the effects of dopant are discussed. The temperature variation of the transition energies has been analyses by the Varshni equation [25] and an expression containing the Bose-Einstein occupation factor for phonons [26,27]. The temperature dependence of the broadening function also has been studied in term of a Bose-Einstein equation that contains the electron (exciton)-longitudinal optical (LO) phonon coupling constant [26,27]. The addition of dopant impurities to a semiconductor is what enables the fabrication of a multitude of interesting devices. The physical role of niobium in influencing the electronic states of the MoS_2 crystal will also be discussed.

2. Experimental

Niobium-doped MoS_2 single crystals have been grown by the chemical vapour transport method with I_2 as a transport agent. The total charge used in each growth experiment was about 10 g. The stoichiometrically determined weight of the doping material was added in the hope that it would be transported at a rate similar to that of Mo. The quartz ampoule containing Br_2 (~5 mg cm^{-3}) and uniformly mixed elements (99.99% pure Mo, Nb and S) was sealed at 10^{-6} Torr. The ampoule was then placed in a three-zone furnace and the charge prereacted for 24 h at 800 ^{0}C with the growth zone at 950 ^{0}C, preventing the transport of the product. The temperature of the furnace was increased slowly to avoid any possibility of explosion due to the exothermic reaction between the elements. The furnace was then equilibrated to give a constant temperature across the reaction tube, and programmed over 24 h to produce the temperature gradient at which single-crystal growth took place. Optimal result were obtained with a temperature gradient of approximately 960 → 930 ^{0}C. Single crystalline platelets up to 10 x 10 mm^2 surface area and 2 mm in thickness were obtained. After 24 h, the furnace was allowed to cool down slowly (40^{0}C/h) to about 200^{0}C.

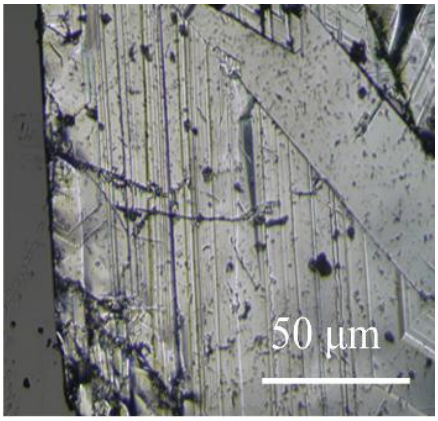

Figure. 1 Photograph of the as-grown niobium-doped MoS_2 single crystal with the surface normal to ***c***-axis

The ampoule was then removed and wet tissues applied rapidly to the end away from the crystals to condense the I_2 vapor. When the ampoule reached room temperature, it was opened and the crystals removed. The crystals were then rinsed with acetone and deionized water. Single crystalline platelets up to 10×10 mm^2 surface area and 2 mm in thickness were obtained. The as-grown niobium-doped MoS_2 single crystal is shown in Fig.1. MoS_2 crystallizes with 2H or 3R structure, while NbS_2 crystallizes in a distorted C6 structure, so that only a small solubility range is to be expected. We do not expect the two solid solutions to be miscible. It was found that a 5% nominal doping of MoS_2 prevented the growth of single crystals.

The PzR measurements were achieved by gluing the thin single crystal specimens on a 0.15 cm thick lead-zirconate-titanate (PZT) piezoelectric transducer driven by a 200 V_{rms} sinusoidal wave at 200 Hz. The alternating expansion and contraction of the transducer subjects the sample to an alternating strain with a typical rms $\Delta l/l$ value of ~ 10^{-5}. A 150 W tungsten-halogen lamp filtered by a model 270 McPherson 0.35 m monochromator provided the monochromatic light. The reflected light was detected by EG&G type HUV-2000B silicon photodiode. The DC output of the silicon photodiode was maintained constant by a servo mechanism of a variable neutral density filter. A dual-phase lock-in amplifier was used to measure the detected signal. Modulated spectra were normalized to the reflectance to obtain $\Delta R/R$. An RMC model 22 close-cycle cryogenic refrigerator equipped with a model 4075 digital thermometer controller was used to control the measurement temperature between 25 and 300 K with a temperature stability of 0.5 K or better.

3. Results and Discussions

Displayed by the dashed curve in Fig. 2 are the PzR spectra near the direct band edge over the range 1.7-2.25 eV for the Au-doped MoS_2 single crystals. The spectra are characterized by two prominent excitonic transitions, A and B excitons. In order to determine the position of the transitions accurately, we performed a theoretical line shape fitting. The energies of both excitonic transitions show the general trend of up-shifting as the temperature is lowered. The linewidths also become narrower in the process. The functional form used in the fitting procedure correspons to a first derivative Lorenzian line shape function of the form [23, 24]

$$\frac{\Delta R}{R} = \mathrm{Re}\left[\sum_{i=1}^{n} A_i^{ex} e^{j\,\ddot{}_i^{ex}} \left(E - E_i^{ex} + j\Gamma_i^{ex}\right)^{-n_i}\right] \quad (1)$$

where A_i^{ex} and $\ddot{}_i^{ex}$ are the amplitude and phase of the line shape, E_i^{ex} and Γ_i^{ex} are the energy and broadening parameters of the inter band excitonic transitions and the value of n_i depend on the origin of the transition. For the first derivative functional form, n = 2.0 is appropriate for the bounded states, such as excitons or impurity transition, while n = 0.5 is applicable for three dimensional critical point inter band transitions [28]. The least-squares fits using equation (1) with $n = 2$ can be achieved and the fits are shown as solid curve in figure 1.The fits yield the parameters A_i, E_i and Γ_i. The obtained values of E_i are indicated as arrows and denoted as A and B. The nomenclature used here follows closely that of Wilson and Yoffe [1] and Beal *et al* [29]. The value of E_i obtained here show a general agreement with slight deviation from the corresponding low temperature transmission data of Beal *et al* [29]. We believed the derivative nature of the PzR spectra should offer better accuracy. The fitted values of E_i are displayed in table 1 together with the relevant works of [29-33] for comparison. The prominent A and B excitons are observed to be red-shifted. The energy position of A and B excitons are measured accurately with the PzR experiment. The splittings of excitons A and B ($\Delta_{BA} = E_B - E_A$) are determined to be 0.16 ± 0.013 eV. These number agreed well with the corresponding previously work [31,32], transmission data of Beal *et all* [29], Reflectance [33], Wavelength modulated reflectance (WMR) spectra of Fortin and Raga and Photoconductivity [30]. In the case of the WMR data of Fortin and Raga, their observed signature, B^* is almost certain to be due to the presence of 3R-MoS_2 in their 2H-MoS_2 sample. From the more recent theoretical and experimental studies [34-36], the A and B excitons are attributed to the smallest direct transitions at the K point of the Brillouin zone split by interlayer interaction and spin-orbit splitting [34, 35]. The A exciton belongs to K_4 to K_5 while the B exciton corresponds to K_1 to K_5 optical transitions. The K states have been shown by Coehoorn *et al* [34, 35] to be predominantly metal *d* states with a small contribution from the non-metal *p* states. According to the figure 2, during growth of Nb-doped MoS_2, the niobium transition ion can interfere between two layer, according to the weak van der Waals forces which link them together. This well known process involves a reduction in stoichiometry, distortion of the crystal structure and/or a variation in the position of the Fermi level. The sandwich Nb ions creates stronger bonds than the original van der Waals forces and converts the two-dimensional structure MoS_2 (2H-MoS_2) of the compound into a three-dimension structure MoS_2 (3R-MoS_2). It is very likely that Nb ions stabilize the 3R polytype of MoS_2. The resulting van der Waals forces of 3R-MoS_2 should be weaker than the 2H polytype and this is reflected by the measured reduction in Δ_{BA}.

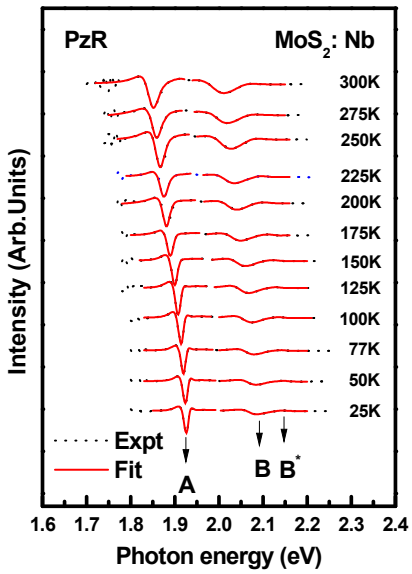

Figure.2. Piezoreflectance spectra of Nb-doped MoS_2 at several temperatures between 25 and 300 K. The dashed curves are the experimental results and the solid curves are least squares fits of Eq. (1).

Table.1 Energies of the excitons A, B and their splitting in MoS_2, MoS_2:Au using equation (1). Relevant values for previously works are included for comparison.

Material	A (eV)	B (eV)	E_{A-B} (eV)	Temperature (K)
MoS_2:Nb [a]	1.928 ± 0.005	2.167 ± 0.008	0.157 ± 0.013	25
	1.920 ± 0.005	2.160 ± 0.008	0.159 ± 0.005	77
	1.852 ± 0.008	2.086 ± 0.01	0.160 ± 0.018	300
MoS_2:Re [b]	1.915	2.066	0.151	15
Undoped MoS_2 [b]	1.928	2.136	0.208	15
MoS_2 [c]	1.88	2.06	0.18	300
MoS_2 [d]	1.9255	2.137	0.2115	4.2
MoS_2 [e]	1.92	2.124	0.204	4.2
MoS_2 [f]	1.929 ± 0.005	2.136 ± 0.008	0.207 ± 0.013	25
	1.845 ± 0.008	2.053 ± 0.01	0.208 ± 0.018	300
2H-MoS_2 [g]	1.910	2.112	0.202	5
3R-MoS_2 [g]	1.908	2.057	0.149	5

[a]Present work.
[b]PzR [31].
[c]Reflectance [33].
[d]WMR [30].
[e]Photoconductivity [30].
[f]PzR [32].
[g]Transmission [29].

4. Summary

In summary we have measured the temperature dependence of the energies and broadening parameters of the direct band-edge excitonic transitions of Nb-doped MoS_2 using PzR in the temperature range 25 to 300 K. From the experimental observations and detailed analysis of

the broadening parameters and energies of the excitonic features A and B, we can infer that the Nb ions are most likely intercalated between the van der Waals gap and stabilize the rhombohedral 3R phase of the MoS_2 crystal instead of forming the ternary $Mo_{1-x}Nb_xS_2$ system. As a result the electronic states of the MoS_2 crystals are modified with a reduction of energy splitting of A and B excitons.

Acknowledgements
The authors would like to acknowledge Professor Ying-Sheng Huang and Professor Ching-Hwa Ho for advising and providing materials and experimental equipment at Semiconductor Characterization Laboratory, National Taiwan University of Science and Technology (NTUST).

References
[1] Wilson J A and Yoffe A D (1969), *Adv. Phys*. **18**, 193
[2] Chang, Y. H. et al. (2013) Highly Efficient Electrocatalytic Hydrogen Production by MoSx Grown on Graphene-Protected 3D Ni Foams. Adv Mater 25, 756–760.
[3] Li, Y. et al. (2011) MoS2 Nanoparticles Grown on Graphene: An Advanced Catalyst for the Hydrogen Evolution Reaction. J Am Chem Soc 133, 7296–7299.
[4] Kong, D. et al. (2013) Synthesis of MoS_2 and $MoSe_2$ Films with Vertically Aligned Layers. Nano Lett 13, 1341–1347.
[5] Kam K K and Parkinson B A, (1982) *J. Phys. Cem*. **86**, 463.
[6] Li S J, Bernede J C, Pouzet J and Jamali M, (1996) *J. Phys.: Condens. Matter* **8**, 2291
[7] Shi, Y. et al. (2012) van der Waals Epitaxy of MoS_2 Layers Using Graphene As Growth Templates. Nano Lett 12, 2784–2791.
[8] Liu, K.-K. et al. (2012) Growth of Large-Area and Highly Crystalline MoS_2 Thin Layers on Insulating Substrates. Nano Lett 12, 1538–1544.
[9] Lin, Y.-C. et al. (2012) Wafer-scale MoS_2 thin layers prepared by MoO_3 sulfurization. Nanoscale 4, 6637-6641.
[10] Lee, Y.-H. et al. (2012) Synthesis of Large-Area MoS_2 Atomic Layers with Chemical Vapor Deposition. Adv Mater 24, 2320–2325.
[11] Zhan, Y., Liu, Z., Najmaei, S., Ajayan, P. M. & Lou, J. (2012) Large-Area Vapor-Phase Growth and Characterization of MoS_2 Atomic Layers on a SiO2 Substrate. Small 8, 966–971.
[12] D. S. Ginley, R. M. Biefeld, B. A. Parkinson and K. Keung-Kam, (1982) J. Electrochem. Soc., 129 145.
[13] A. Casalot, M. Chaouch and G. Vacquier, Ann. (1986) ('him.Fr., 11 509.
[14] Radisavljevic, B., Radenovic, A., Brivio, J., Giacometti, V. & Kis, A. (2011) Single-layer MoS2 transistors. Nat Nano 6, 147–150.
[15] Lembke, D. & Kis, A. (2012) Breakdown of High-Performance Monolayer MoS_2 Transistors. ACS Nano 6, 10070–10075.
[16] Wang, H. et al. (2012) Integrated Circuits Based on Bilayer MoS_2 Transistors. Nano Lett 12, 4674–4680.
[17] Eda, G. et al. (2011) Photoluminescence from Chemically Exfoliated MoS_2. Nano Lett 11, 5111–5116.
[18] Splendiani, A. et al. (2010) Emerging Photoluminescence in Monolayer MoS_2. Nano Lett 10, 1271–1275.
[19] R. Murray, B.L. Evans, (1979) J. Appl. Crystallogr. **12** 312.

[20] Clark A H 1970 N. Jahrbuchf. Mineral. Monatsheffe **3** 33
[21] J. B Legma, G. Vacquier, Traorè and A. casalot, 1991 Mater. Sci. Eng. B **8** 167.
[22] Mathieu H, Allegre J and Gil B, (1991) *Phys. Rev*. B **43**, 2218
[23] Pollak F H and Shen H, (1993) *Mater. Sci. Eng*. R **10**, 275
[24] Aspnes D E 1980 *Optical Properties of Semiconductors (Handbook on Semiconductors 2)* ed M Balkanski (Amsterdam: North-Holland) p 109
[25] Varnish Y P, (1967) *Physica* **34**, 149
[26] Lantenschlager P, Garriga M, Logothetidis S and Cardona M, (1987) *Phys. Rev*. B **35**, 9178
[27] Lantenschlager P, Garriga M, Vina L and Cardona M, (1987) *Phys. Rev*. B **36**, 4821
[28] Aspnes D E 1980 *Optical Properties of Semiconductors (Handbook on Semiconductors 2)* ed M Balkanski (Amsterdam: North-Holland) p 109
[29] Beal A R, Knights J C and Liang W Y, (1972) *J. Phys. C: Solid State Phys*. **5,** 3540
[30] Fortin E and Raga F, (1975) *Phys. Rev*. B **11**, 905
[31] Malikova L, Krystek W, Pollak F H, Dai N, Cavus A and Tamorgo M C, (1996) *Phys. Rev*. **B** 54, 1819
[32] Qiang H, Pollak F H, Sotomayor Torres C M, Leitch W, Kean A H, Stroscio M, Jafrate G J and Kim K W, (1992) *Appl. Phys. Lett*. **61**, 1411
[33] Beal A R, Liang W Y and Huges H P, (1976) *J. Phys. C: Solid State Phys*. **9,** 2449
[34] Coehoorn R, Haas C, Dickstra J, Flipse C J F, de Groot R A and Wold A, (1987) *Phys. Rev*. B **35**, 6195
[35] Coehoorn R, Haas C, and de Groot R A, (1987) *Phys. Rev*. B **35**, 6203
[36] Straub Th, Fauth K, Finteis Th, Hengsberger M, Claessen R, Steiner P, Hufner S and Blaha P, (1996) *Phys. Rev*. B **53**, 16152